NONLINEAR ANALYSIS OF INTERHEMISPHERIC CONNECTIVITY IN THE PENTYLENETETRAZOL RAT MODEL OF SPIKE-WAVE DISCHARGES

Anastasia A. Grishchenko

Peter the Great St. Petersburg Polytechnic University St. Petersburg, Russia Saratov State University Saratov, Russia vili_von@mail.ru

Anastasia S. Dzhafarova

Peter the Great St. Petersburg Polytechnic University St. Petersburg, Russia Saratov State University Saratov, Russia dzhafarovaan@gmail.com

Elena M. Suleymanova

Institute of Higher Nervous Activity and Neurophysiology of Russian Academy of Sciences Moscow, Russia e.m.suleymanova@gmail.com

Marina V. Sysoeva

Peter the Great St. Petersburg Polytechnic University St. Petersburg, Russia bobrichek@mail.ru

Ilya V. Sysoev

Peter the Great St. Petersburg Polytechnic University St. Petersburg, Russia Saratov State University Saratov, Russia ivssci@gmail.com

Article history:

Received 15.06.2025, Accepted 19.09.2025

Abstract

Diagnostics of epileptic activity is usually based on visual and/or automated analysis of brain electromagnetic signals, including EEGs, MEGs, local field potentials and single/multi neuron unit recordings. In primary generalized epilepsies the pathological activity is detected in both hemispheres. However, in some animal models this was not tested properly. Recently, we have found that in pentylenetetrazol rat model of spike-wave discharges (SWDs) in half of subjects a significant part of SWDs was expressed in the cortex of only one hemisphere. The purpose of this paper is to test whether such discharges differ from background activity. In this paper we use both indirected (phase coherence index, mutual information function) and directed (nonlinear adapted Granger causality) nonlinear measures which became popular in neuroscience last decades. Studying connectivity changes accompanying discharge initiation we found increase in interhemispheric coupling similar to that found previously between different cortical regions of the same hemisphere, with no specific preictal connectivity dynamics distinguishable. We also showed that there was no significant difference in interhemispheric connectivity between unilaterally and bilaterally expressed discharges. In pentylenetetrazol rat model of SWDs there is a significant increase in connectivity between hemispheres of somatosensoty cortex during ictal

stage. This increase is expressed at the same level for both unilaterally and bilaterally visible discharges.

Kev words

Brain connectivity, rat model, spike-wave discharges, nonlinear analysis, pentylenetetrazol, phase coherence index, mutual information function, adapted nonlinear Granger causality.

1 Introduction

Absence epilepsy is usually manifested in spontaneous recurrent spike-wave discharges (SWDs) recorded in both scalp EEG and intracranial brain local field potentials (LFPs). Both thalamus and cortex play significant role in SWD generation [Russo et al., 2016]. Animal models (mostly strains of genetic models: WAG/Rij rats [Coenen and van Luijtelaar, 2003] and GAERS rats [Vergnes et al., 1987]) play the extremely important role in investigation of absence epilepsy since they provide possibility to measure all necessary brain structures with high signal quality. Since SWDs are always considered as primary generalized discharges [Berg et al., 2010; Scheffer et al., 2017], their recording in rat models is usually done from a single hemisphere. This approach allowed to investigate involvement of different thalamic nuclei [Lüttjohann and van Luijtelaar, 2012] and cortical

regions [van Rijn et al., 2010]. However, this also made a large time gap in investigation of crosshemisphere interactions accompanying SWDs from very early works [van Luijtelaar and Coenen, 1986]. Coupling between different brain structures of the same hemisphere was studied using modern techniques such as transfer entropy [Schreiber, 2000], phase coherence index [Mormann et al., 2000] or nonlinear adapted Granger causality [Marinazzo et al., 2006; Kornilov et al., 2016], see [Lüttjohann and van Luijtelaar, 2012; Sysoeva et al., 2014; Lüttjohann and van Luijtelaar, 2015; Sysoeva et al., 2016b; Sysoeva et al., 2016c] for instance. In contrary, dynamics of interhemispheric connectivity accompanying SWDs in rats remains mostly unclear. The main reason for this is that most modern techniques for connectivity detection were developed for last 25 years, i.e. at the time when synchronous pathological activity in both hemispheres during SWDs was considered to be proven and therefore, signals from both hemispheres were not measured from SWD models.

In addition to genetic models, pharmacological induction of SWDs is used sometimes. The main advantage of the pharmacological models is the possibility to obtain measurements from the same animal before and after initiation of absence-like activity. Administration of low doses of the popular proepileptic drug pentylenetetrazole (PTZ) leads to generation of recurrent SWDs in different rodents: rats [Marescaux et al., 1984], mice [Medina et al., 2001] and guinea pigs [Solmaz et al., 2009], though higher doses of the same substance cause tonic-clonic seizures [Klioueva et al., 2001]. It is interesting that there is a single work [Myslobodsky and Rosen, 1979] pointing to possible asymmetry in SWD development for PTZ invoked seizures. In this paper, the authors counted number and length of seizures and established that asymmetry as well as symmetry in the seizure length (or even existence) are both typical.

In our previous research, we found that PTZ-induced SWDs can appear in only one or in both hemispheres [Ershova et al., 2023] supporting the results published in [Myslobodsky and Rosen, 1979]. The effect was even more complex: some animals mainly exhibited bilaterally symmetric SWDs while others showed both symmetric and asymmetrically developed SWDs up to the cases when SWD in one hemisphere was absent. All cases could be recorded in a single animal. Therefore, further we assume that asymmetric discharges are discharges differed in length and amplitude in two hemispheres including the case when there is no discharge in one of hemispheres. In our case these results were obtained using automatic seizure detection algorithm with such algorithms being developed for SWD detection last decades and unavailable in 1979 (so the authors of [Myslobodsky and Rosen, 1979] were to count seizures by eye).

Since SWDs are usually the result of pathological synchronous activity of the entire thalamocortical system, it

is necessary to answer whether the observed differences in the SWD pattern are the result of crosshemispheric connectivity dynamics, or this is a result of some local neural activity preventing the appearance of SWDs in one hemisphere. However, to consider this issue we have to determine what are the coupling differences between discharges and background activity, as it was investigated for inrahemispheric connections. To answer this question, we used a number of methods for connectivity estimation: phase synchronization index [Mormann et al., 2000], mutual information function calculated following nearest neighbors approach [Kraskov et al., 2004] and nonlinear adapted Granger causality with polynomial functions [Sysoeva et al., 2014; Kornilov et al., 2016] and models constructed based on BIC criterion [Schwarz, 1978]. Use of mostly nonlinear methods is based on the idea that SWDs are highly nonlinear phenomenon in which second harmonic of the main rhythm (and also higher ones) may be as much valuable as the first one, with nonlinear interaction between signal components on different frequencies being able to significantly contribute to the connectivity [Dolinina et al., 2024]. The recent theoretical studies for different quadratic and cubic nonlinearities [Turukina, 2024] show that interactions between modes in different ranges (actually, their higher harmonics) may play significantly effects the regime of oscillations in the networ.

Actually, the used measures assume that the considered signals are generated by some nonlinear oscillator. So, the alternative approach is to write out some differential equations describing the system and adjust their parameters to the data as it was proposed previously using both methods of adaptive control [Plotnikov, 2024] and system identification [Sysoev and Bezruchko, 2021]. We skipped these approaches here since they rely very heavily on a specific type of model which is unknown for the considered case.

2 Data and methods

2.1 Experimental data

Experiments were performed on male Wistar rats, 6-7 months of age, obtained from the Stolbovaya Animal Breeding Center (Moscow). Electrical activity of the neocortex was recorded using electrodes (steel screws) implanted in symmetrical areas of the frontal cortex of both hemispheres at the coordinates: AP 2; ML ± 2 ; DV 1 [Paxinos and Watson, 2006]. A steel screw located above the cerebellum was used as an indifferent electrode. The electrodes were implanted under anesthesia (chloral hydrate, 380 mg/kg) two weeks before the experiments. Electrical activity of the cortex was recorded using a 4-channel amplifier and an ADC (E14-440, LCard, Russia) in awake freely moving animals. Intraperitoneal injection of the convulsant PTZ at a dose of 40 mg/kg was used to induce spike-wave dis charges. At the end of the experiment, histological analysis was per-

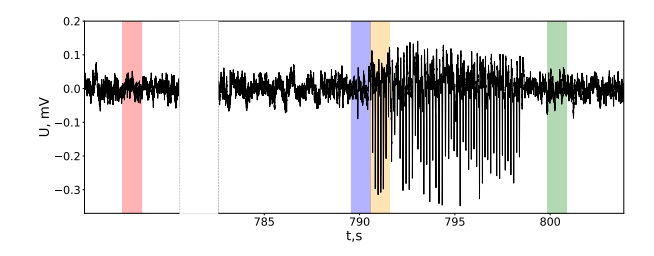


Figure 1. Example of discharge in rat models of epilepsy. The colored bars on the graph show the intervals for which the connectivity was analyzed: red color — one second of background activity, blue color — one second exactly before the seizure start (preictal epoch), orange color — one second just after the seizure start (ictal epoch) and green color — one second just after the seizure end (postictal or maybe background activity).

Table 1. Number of symmetric and asymmetric discharges.

Rat No.	1	3	5	7	8	9
Symmetric	4	5	27	27	27	27
Asymmetric	4	5	23	27	8	13
Total	8	10	50	54	35	40

formed to determine the localization of recording electrodes.

In the present work, recordings of six animals were considered; the duration of all recordings was at least 1 h, being 90 min in average. We chose these six animals from nine reported previously [Ershova et al., 2023] due to they have both symmetric and asymmetric discharges, see Table 1. To make the bridge to the previous study, we preserved the numbers of animals, therefore animals No. 2, 4 and 6 are absent. The discharges were detected using the automated approach proposed in [Ershova et al., 2023].

Several intervals were chosen to compare discharge with background activity. They are shown in the Fig. 1: one second of background activity, one second before the start of discharge (preictal epoch), 1one second after the start of discharge (ictal epoch) and one second after the end of discharge (postictal epoch).

The typical discharges with spectrograms are plotted in Fig. 2. These series and spectrogram have a number of similarities with series and spectrograms of genetic rat models. First, the main frequency is about 6.5–7 Hz for all considered animals which is very close to what is known for GAERS rats as it was mentioned previously [Marescaux et al., 1984]. Second, one can see up to five harmonics of the main frequency in both hemispheres, which is very similar to what is known from genetic models [Coenen and van Luijtelaar, 2003; Vergnes et al., 1987], with very similar plots for different channels from the single hemisphere of WAG/Rij rats being published in [Sysoeva et al., 2016c]. Third, there

is a slow decrease of the main frequency which may be better seen when following the dynamics of the second and, especially, third harmonic during the discharge, see Fig. 2 c,d. The similar decrease was also detected for WAG/Rij rats in many works [Lüttjohann and van Luijtelaar, 2015]. Forth, the amplitude of SWDs in the considered model is from two to six times higher than for background activity, matching what was found for genetic models.

2.2 Phase coherence index

The phase coherence index $I_{x,y}$ is a very popular measure of signal similarity proposed in [Mormann et al., 2000]. First, one has to establish signal phases φ_x and φ_y for both observed signals (time series) $\{x_i\}_{i=1}^N$ and $\{y_i\}_{i=1}^N$ respectively. To do this, Hilbert–Huang transform is usually applied [Huang et al., 1998] to both signals separately, with other approaches also being possible. Then, the index $I_{x,y}$ is calculated as follows:

$$I_{x,y} = \left| \left\langle \exp\left(j(\varphi_x(t_i) - \varphi_y(t_i))\right) \right\rangle_{i=1,\dots,N} \right|, \quad (1)$$

where j stays for imaginary unit.

If the phases φ_x and φ_y behave completely independently (no phase synchrony at all), the difference $\varphi_x(t_i)-\varphi_y(t_i)$ is distributed uniformly over the semi-interval $[0;2\pi)$, and $I_{x,y}\to 0$ for $N\to\infty$. If the difference $\varphi_x(t_i)-\varphi_y(t_i)=\mathrm{const}\ \forall i$, then $I_{x,y}=1$ (complete synchrony). If there is some nonuniform distribution of $\varphi_x(t_i)-\varphi_y(t_i)$ with some maximum, we obtain $0< I_{x,y}<1$, reaching some nonzero value (partial synchrony).

It must be noted that $I_{x,y}$ actually reveals signal phase synchrony despite of its reason. Both bidirectional and unidirectional coupling leading to synchronization and synchronization by means of external driving may lead to similar values. Also, there is no safe way to detect the coupling direction by this measure, as it was shown in [Vakorin et al., 2013].

2.3 Mutual information function

The mutual information function $MI_{x,y}$ between two samplings (in our case — time series) $\{x_i\}_{i=1}^N$ and $\{y_i\}_{i=1}^N$ characterizes the degree of series similarity. Actually, it is a best way to estimate the nonlinear similarity of two time series if frequency resolution is not necessary or cannot be obtained due to insufficient data. The primary formula for calculation of $MI_{x,y}$ is based on its definition by means of individual and joint entropies:

$$MI_{x,y} = H_x + H_y - H_{x,y}.$$
 (2)

Since straightforward approaches based on splitting the phase space into bins are very inefficient we used the technique proposed in [Kraskov et al., 2004] which operates with Kazachenko–Leonenko entropy [Kozachenko and Leonenko, 1987] and uses nearest neighbour count

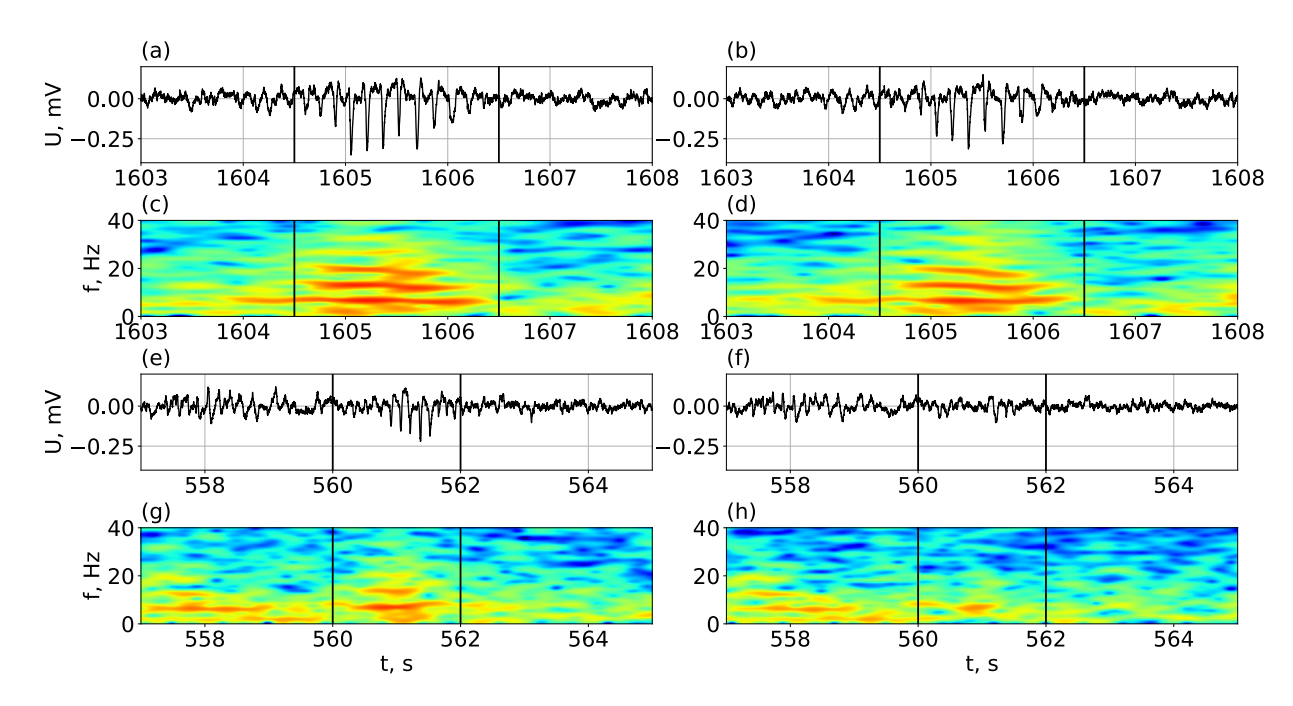


Figure 2. Example of symmetrical and asymmetrical discharges in a rat models of epilepsy. The subfigs. (a,b) show a time series of local field potentials for symmetrical discharge from the left (a) and right (b) brain hemispheres recorded from frontal cortex, the subfigs. (c,d) are spectrograms for these discharges. The subfigs. (e,f) show a time series of local field potentials for asymmetrical discharge from the left (e) and right (f) brain hemispheres recorded from frontal cortex, the subfigs. (g,h) are spectrograms for these discharges.

to construct the estimator. The calculation formula (3) is as follows:

$$MI_{x,y} = \psi(N) + \psi(K) - \langle \psi(n_x(i) + 1) + \psi(n_y(i) + 1) \rangle_{i=1,\dots,N},$$
(3)

where N is the series length (sampling size), K is the number of the neighbor (the simplest choice is K=1), $n_x(i)$ and $n_y(i)$ are the numbers of "partial" neighbors of the i-th point by X or Y direction only, $\psi(n)$ is digamma function.

2.4 Adapted nonlinear Granger causality

The adapted nonlinear Granger causality method was used here as a primary tool for directed connectivity estimation. This method was proposed specifically for the absence seizure study in [Sysoeva et al., 2014]. In general, the idea to adapt the mathematical models and methods from different fields to specifics of neuroscience was discussed multiple times (see the recent review [Babich et al., 2025] for details). The method is based on construction of empirical predictive models in the time window, adopting the ideas from [Hesse et al., 2003], but using nonlinear models of the form (4) with specially selected parameters.

$$x'_{n+\tau} = f(x_n, x_{n-l}, \dots, x_{n-(D_s-1)l}),$$
 (4)

where $x'_{n+\tau}$ is the predicted value corresponding to the measured value $x_{n+\tau}$, f is a general polynomial of order P from D_s variables, $\mathbf{x}_n = (x_n, x_{n-l}, ..., x_{n-(D_s-1)l})$

is a state vector as defined by means of the method of delays [Packard et al., 1980].

Method of delays is a classical approach to reconstruct the high-dimensional state vector $\{\mathbf{x}_n\}_{n=1}^{N-(D_s-1)l}$ from the scalar time series $\{x_n\}_{n=1}^N$ by shifting this series back in time. To obtain a D-dimensional vector one has to make (D_s-1) times shifts with a lag l. Unfortunately, this approach usually leads to very large model with many coefficients, which cannot be reliably estimated from the provided data. in [Kugiumtzis, 1996] it was shown that nonuniform embedding (using different lags for each time shift) may significantly reduce the model dimension. Another possible way to solve this problem is using a separate prediction length parameter τ [Sysoeva and Sysoev, 2012], which is the time interval between the last data point used for vector reconstruction and the point to be predicted. To estimate the model dimension and the polynomial order D we used Bayesian information criterion [Schwarz, 1978]. Model coefficients were estimated using the least-squares routine by minimising the squared prediction error (4), that measures the difference between the predicted values $x'_{n+\tau}$ and the observed ones $x_{n+\tau}$:

$$\varepsilon_s^2 = \frac{1}{N'\sigma_s^2} \sum_{n=(D_s-1)l}^{N-\tau} (x'_{n+\tau} - x_{n+\tau})^2 \to \min, \quad (5)$$

where σ_s^2 is the variance of the time series $\{x_n\}_{n=1}^N$, $N' = N - \tau - (D_s - 1)l$ is the efficient length of the time series.

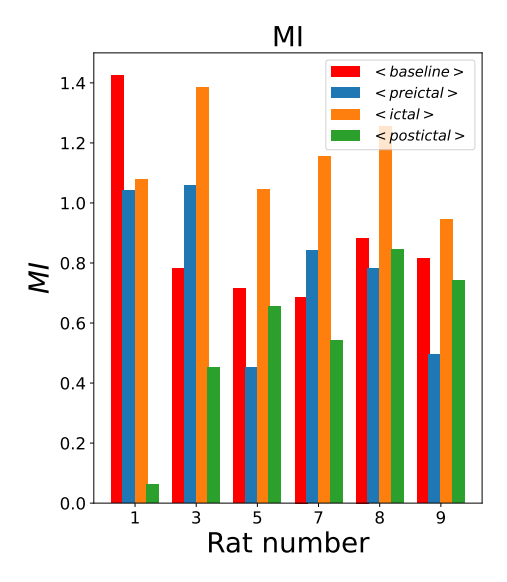


Figure 3. Histogram of mean values MI for baseline activity (red), preictal activity (blue), ictal activity (orange), and postictal activity (green).

Second, a bivariate model (6) was constructed from both time series $\{x_n\}_{n=1}^N$ and $\{y_n\}_{n=1}^N$:

$$x''_{n+\tau} = g\left(x_n, x_{n-l}, \dots, x_{n-(D_s-1)l}, y_n, \dots, y_{n-(D_a-1)l}\right),$$
(6)

where g is a general polynomial of the order P (the same as for the model (4)), D_a is a dimension of the state vector $\mathbf{y}_n = \left(y_n, y_{n-l}, y_{n-(D_a-1)l}\right)$ reconstructed from the scalar time series $\{y_n\}_{n=1}^N$. So, the total dimension of the bivariate model can be computed as $D_j = D_s + D_a$, and its squared prediction error is denoted as ε_j^2 .

Third, the value of the prediction improvement PI, that is considered as a main characteristic of the Granger causality method, was computed following (7).

$$PI = 1 - \frac{\varepsilon_j^2}{\varepsilon_s^2},\tag{7}$$

In this study, several sets of parameters satisfying the criteria from [Sysoeva and Sysoev, 2012; Sysoeva et al., 2012; Kornilov et al., 2016] were tested to find the optimal sensitivity/specificity ratio. As a result, the prediction length was empirically chosen to be $\tau=T/8$, where T is a main time scale of oscillations. For absence seizures, for which the main frequency is usually from 6 Hz to 9 Hz, so $0.11 \lesssim T \lesssim 0.17$ s. The other parameters were chosen automatically according to the Schwarz's (BIC) criterion [Schwarz, 1978]: the dimension of the individual model $D_s=4$, the polynomial order P=2, and the lag in the model l=T/6. The calculations were carried out in non overlapping time windows of two seconds length (2000 discrete values, about 16 characteristic periods).

The coefficient of prediction improvement $(PI \in$ [0; 1]) is used as a mathematical characteristic of Granger causality. Prediction improvement PI = 0 corresponds to no coupling in the considered direction, $PI \rightarrow 1$ corresponds to the case when all possible coupling terms are taken into account properly. Theoretically, the situations PI = 0 and PI = 1 are achievable, but in such a case the model structure should describe the object completely [Kornilov et al., 2016]. Practically, values 0 < PI < 1 are obtained for both presence and absence of actual coupling. The main reasons of such method imperfection are finite time resolution [Smirnov, 2014], incorrect choice of method parameters, finite series length, noise, complex nonlinearity in the studied system and other factors [Smirnov, 2013]. Therefore, it is usually stated that an absolute value of PI carries little information about the degree of connectivity. However, using the same model throughout the study, interpretation of increase or decrease of PI makes sense, with providing possibilities to track changes in connectivity accompanying different processes in the brain.

2.5 Statistical evaluation of connectivity estimates

To quantitatively describe differences in the duration of discharges, we used two well known statistical tests: the Kolmogorov–Smirnov test (further, KS-test for brevity) and the Mann–Whitney test (further, MW-test for brevity). Both approaches test the hypothesis that two samples are taken from the same distribution. Both methods produce a p-value, the probability of being wrong, refuting the hypothesis that the distributions are the same. Generally, when p-values are small, the conclusion is made that the differences are significant, while when p-values are relatively large, for example, p > 0.05, the initial hypothesis is accepted and the samples are considered to belong to the same distribution. All calculation were performed using scipy.stats framework [Virtanen et al., 2020].

3 Results

3.1 Searching for connectivity during discharges and background activity

We applied the nonlinear adapted Granger causality and mutual information function to four intervals: background activity (colored in red in Fig. 1), preictal activity (colored in blue in Fig. 1), ictal activity (colored in orange in Fig. 1), and postictal activity (colored in green in Fig. 1). Mean values $\langle PI \rangle$ and $\langle MI \rangle$ averaged over all episodes for each rat separately are presented in the table 2 and in Fig. 4 for nonlinear adapted Granger function and Fig. 3 for mutual information function.

Analyzing results of mutual information function calculation, it can be concluded that the discharge is different at the level p=0.01 and lower from the background in almost all rat, except in rat No. 1 for which no significance difference detection can be explained by

Table 2. Mean values for the nonlinear adapted Granger causality and mutual information function.

	1	3	5	7	8	9		
GC L-R								
baseline	0.07	0.02	0.02	0.03	0.06	0.01		
preictal	0.07	0.07	0.03	0.01	0.05	0.02		
ictal	0.18	0.05	0.07	0.11	0.10	0.15		
postictal	0.04	0.03	0.03	0.01	0.03	0.03		
GC R-L	GC R-L							
baseline	0.07	0.03	0.03	0.02	0.03	0.03		
preictal	0.05	0.07	0.02	0.02	0.04	0.03		
ictal	0.07	0.07	0.10	0.07	0.07	0.07		
postictal	0.04	0.05	0.01	0.02	0.01	0.02		
MI								
baseline	1.43	0.78	0.71	0.69	0.88	0.81		
preictal	1.04	1.06	0.45	0.84	0.78	0.50		
ictal	1.08	1.38	1.04	1.15	1.25	0.95		
postictal	0.06	0.45	0.65	0.54	0.85	0.74		

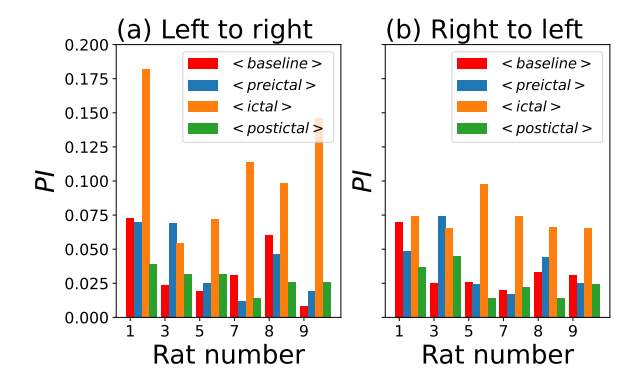


Figure 4. Histogram of mean values of PI for baseline activity (red), preictal activity (blue), ictal activity (orange), and postictal activity (green). The subfig. (a) shows PI in the direction from left to right, the subfig. (b) — in the direction from right to left.

a small number of discharges, see Tab. 3. This result is in a good correspondence with what was previously obtained for genetic rat models when considering connectivity dynamics between different areas of neocortex in a single hemisphere [Sysoeva et al., 2016c; Sysoeva et al., 2016a]. At the same time, there is no significant difference between preictal and background activity. Since for three of six considered rats MI for background even larger than for preictal, see Tab. 2, this fact

is unlikely due to insufficient data. There could be two main explanations: first is that preictal changes in connectivity dynamics which are actually responsible for SWD initiation are mostly localized inside the particular hemisphere. This means that thalamocortical loops in both hemispheres act mostly independently, but with the same main dynamical patterns. Such an explanation well matches the modern concepts of SWD mechanisms which consider intrahemispheric couplings to be enough for SWD initiation [Lüttjohann and van Luijtelaar, 2015]. The other explanation is that interhemispheric changes in PTZ model are different to those in the genetic ones and humans; this thesis may be considered only by new experimental research with genetic models.

The results of the Granger causality mostly support the outcomes obtained using the mutual information function. First, if one excludes the rat No. 1 due to insufficient data, both statistical test indicate significant and bidirectional increase in coupling during SWDs in comparison to background (the only exception is MW-test i the direction from right to left for rat No. 3, for which p = 0.1). For Granger causality, the significance level is even higher $(p \le 10^{-3})$ than for the mutual information function. This matches well the previous investigations in which WAG/Rij rats were considered [Sysoeva et al., 2016b]. Second, the KS test (which is more conservative and usually requires more data) does not provide significant differences between connectivity in background time and in the preictal epoch, as was shown using the mutual information function, the MW-test (which is usually considered to be more sensitive for small samplings) indicated significant increase in coupling in both directions for the rat No. 3 and significant decrease in one direction for the rat No. 7 at the level $p = 10^{-3}$. Since the sampling for the rat No. 3 is relatively small, this may be an artifact of the method.

3.2 Search for connectivity in asymmetric discharges

First of all, we applied the mutual information function to both types of discharges activity to study the signal similarity between homotopic cortical regions of two hemispheres. The mean values $\langle MI \rangle$ averaged over all episodes for each rat separately are presented in Table 4 (first and second rows are for symmetric and asymmetric discharges, respectively, while the fifth row is for the baseline activity) and in Fig. 5a. The values obtained for symmetric and asymmetric discharges can be different, but all of them lie in the same range. Statistical test: The Kolmogorov–Smirnov test (third row in the table 4) and the Mann-Whitney test (fourth row in the table 4) indicate that the obtained MI values cannot be considered as belonging to different distributions with p-value being > 0.1 for all animals for both tests. This means that using mutual information we cannot detect any difference in signal similarity between the considered signals from

Statistical tests for the nonlinear adapted Granger Causanty and mutual information ful								
	1	3	5	7	8	9		
GC L-R								
KS-preictal	0.7	0.2	0.8	0.4	0.8	0.6		
MW-preictal	0.3	10^{-3}	0.5	10^{-3}	0.5	0.01		
KS-ictal	0.9	10^{-10}	10^{-3}	10^{-13}	10^{-8}	10^{-10}		
MW-ictal	0.3	10^{-13}	10^{-5}	10^{-10}	10^{-10}	10^{-10}		
KS-postictal	0.2	0.7	0.5	0.5	0.5	0.2		
MW-postictal	10^{-3}	0.5	0.2	0.2	0.2	10^{-5}		
GC R-L								
KS-preictal	0.3	0.1	0.9	0.9	0.9	0.9		
MW-preictal	0.1	10^{-3}	0.5	0.5	0.5	0.5		
KS-ictal	0.9	0.1	10^{-5}	10^{-10}	10^{-10}	10^{-10}		
MW-ictal	0.5	10^{-3}	10^{-6}	10^{-10}	10^{-10}	10^{-10}		
KS-postictal	0.01	0.01	0.5	0.9	0.8	0.9		
MW-postictal	10^{-3}	10^{-3}	0.3	0.8	0.5	0.8		
MI								
KS-preictal	0.5	0.5	0.1	0.3	0.2	0.2		
MW-preictal	0.3	0.3	0.1	0.1	0.2	0.1		
KS-ictal	0.2	10^{-5}	10^{-9}	10^{-9}	10^{-5}	0.01		
MW-ictal	0.1	10^{-5}	10^{-12}	10^{-11}	10^{-5}	0.01		
KS-postictal	10^{-3}	0.8	0.7	0.9	0.9	0.2		
MW-postictal	10^{-5}	0.5	0.3	0.8	0.8	0.1		

Table 3. Statistical tests for the nonlinear adapted Granger causality and mutual information function.

Table 4. Testing for equality distributions of mutual information function $\langle MI \rangle$ obtained for symmetric SWDs $\langle MI_s \rangle$, asymmetric SWDs $\langle MI_a \rangle$ and baseline activity $\langle MI_b \rangle$. KS-test_d means Kolmogorov–Smirnov test for discharges, KS-test_b means Kolmogorov–Smirnov test for baseline activity, MW-test_d means Mann–Whitney test for discharges, MW-test_b means Mann–Whitney test for baseline activity.

Rat No.	1	3	5	7	8	9
$\langle MI_s \rangle$	1.05	1.32	1.14	1.08	1.11	0.75
$\langle MI_a \rangle$	1.29	1.22	1.27	1.12	1.22	0.89
KS-test _d	0.70	0.80	0.10	0.30	0.20	0.20
MW-test _d	0.30	0.50	0.10	0.10	0.20	0.10

two hemispheres, though the signal shape and amplitude differ significantly.

Since MI did not reveal the difference in connectiv-

ity between symmetric and asymmetric discharges, we calculated phase synchronization index. Unfortunately, this could not be done for the baseline activity since there was no possibility to establish a phase properly (the baseline activity does not have one main frequency). The results were presented in Table 5 and in Fig. 5b. One can see that PS also reveals no difference between symmetric and asymmetric discharges with $p \ge 0.2$ based on both the Kolmogorov-Smirnov and Mann-Whitney tests. This is interesting due to the fact that in the asymmetric discharges there was no oscillation shape typical for SWDs in one hemispheres. Nevertheless, the frequency of the main rhythm occurred to be same in both channels, providing possibility to establish the phase. And the results were statistically indistinguishable with $p \ge 0.1$.

Since non-directional methods were not able to reveal the difference in interhemispheric connectivity between symmetric and asymmetric discharges, we applied nonlinear adapted Granger causality following the pa-

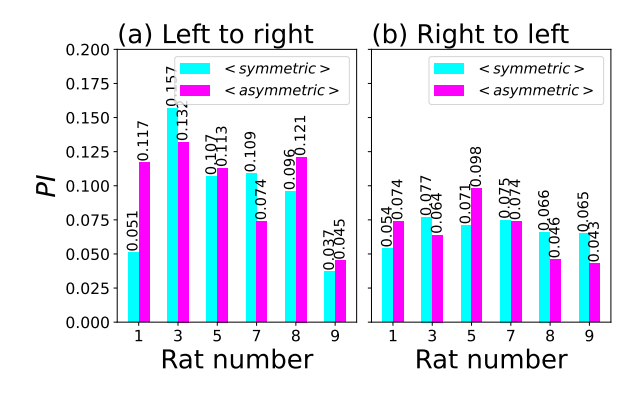


Figure 6. Histogram of mean values PI for symmetric discharges (blue) and asymmetric discharges (pink). The subfig. (a) shows PI in the interhemispheric connectivity estimates for the direction from left to right, the subfig. (b) — in the direction from right to left.

Table 7. Testing for equality distributions of prediction improvement $\langle PI_{\rangle}$ obtained for symmetric discharges $\langle PI_{s} \rangle$, asymmetric discharges $\langle PI_{a} \rangle$ and baseline activity $\langle PI_{b} \rangle$. KS-test_d means Kolmogorov–Smirnov test for discharges, KS-test_b means Kolmogorov–Smirnov test for baseline activity, MW-test_d means Mann–Whitney test for discharges, MW-test_b means Mann–Whitney test for baseline activity. PI values were obtained using nonlinear adapted Granger causality in the direction from right to left hemisphere.

Rat No.	1	3	5	7	8	9
$\langle PI_s \rangle$	0.05	0.08	0.07	0.08	0.07	0.07
$\langle PI_a \rangle$	0.07	0.06	0.10	0.07	0.05	0.04
KS-test _d	0.10	0.30	0.40	0.90	0.10	0.10
MW-test _d	0.20	0.20	0.10	0.80	0.10	0.10

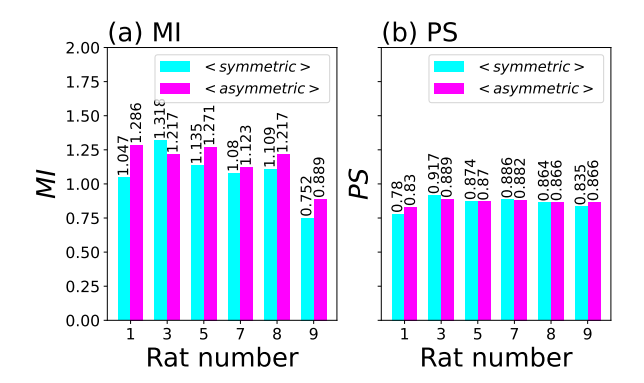


Figure 5. Histogram of mean values MI in (a) and PS in (b) for symmetric discharges (blue) and asymmetric discharges (pink).

Table 5. Testing distributions of phase synchronization index estimates $\langle PS \rangle$ obtained for symmetric $\langle PS_s \rangle$ and asymmetric $\langle PS_a \rangle$ discharge for equality. KS-test_d means Kolmogorov–Smirnov test for discharges, MW-test_d means Mann–Whitney test for discharges.

Rat No.	1	3	5	7	8	9
$\langle PS_s \rangle$	0.78	0.92	0.87	0.89	0.86	0.84
$\langle PS_a \rangle$	0.83	0.89	0.87	0.88	0.87	0.87
KS-test _d	0.80	0.30	0.90	0.70	0.80	0.50
MW-test _d	0.70	0.20	0.70	0.80	0.90	0.30

Table 6. Testing for equality distributions of prediction improvement $\langle PI \rangle$ obtained for symmetric discharges $\langle PI_s \rangle$, asymmetric discharges $\langle PI_a \rangle$ and baseline activity $\langle PI_b \rangle$. KS-test_d means Kolmogorov–Smirnov test for discharges, KS-test_b means Kolmogorov–Smirnov test for baseline activity, MW-test_d means Mann–Whitney test for discharges, MW-test_b means Mann–Whitney test for baseline activity. PI values were obtained using nonlinear adapted Granger causality for left to right discharge.

Rat No.	1	3	5	7	8	9
$\langle PI_s \rangle$	0.05	0.16	0.11	0.11	0.10	0.04
$\langle PI_a \rangle$	0.12	0.13	0.11	0.07	0.12	0.05
KS-test _d	0.40	0.80	0.80	0.50	0.40	0.20
MW-test _d	0.50	0.80	0.80	0.50	0.60	0.20

per [Sysoeva et al., 2014]. The idea was that the mutual information and phase synchronization index estimates might be similar for symmetric and asymmetric discharges because both unidirectional and bidirectional coupling was able to provide the same level of signal similarity or synchrony.

The results from the tables 6 and 7 were also plotted in Fig. 6, where the mean PI values from left to right were shown in the subplot (a) and from right to left — in the subplot (b).

Though Granger causality occurred to be able to detect changes in connectivity caused by discharge, there was no significant connectivity difference between symmetric and asymmetric discharges, indicating that even the specialized nonlinear directed approach was not able to detect connectivity difference. This may mean that the difference in the signal shape between symmetric and asymmetric discharges is a result of different intrahemispheric connectivity in two hemispheres rather than crosshemipheric interactions. To address this issue one have to measure more signals from both hemishperes (three or more symmetric channels) to be able to detect and describe differences in intrahemispheric connectivity as well as control the signal asymmetry.

4 Conclusions and discussion

First, we found that crosshemispheric connectivity in the neocortex significantly increased during pharmacologically induced SWDs in comparison to baseline activity. This increase is similar to what was previously found for intrahemispheric cortical connectivity in genetic model of absence epilepsy [Sysoeva et al., 2016c]. At the same time, there was no statistically reliable increase for preictal epoch (two seconds before the SWD). Absence of the preictal connectivity increase may be caused by fundamental factors, since thalamocortical loop responsible for SWDs is usually considered to work independently in both hemispheres [Coenen and van Luijtelaar, 2003], with crosshemispheric interactions being the secondary effect. However, this issue needs additional investigation using simultaneous recordings from thalamic nuclei and somatosensory cortex in both hemispheres.

Second, we found that there is no significant difference in coupling estimates between SWDs symmetrically expressed in both hemispheres and SWDs expressed only in one hemisphere. Since we used three different connectivity measures this means that interhemispheric connectivity is insufficient for SWD expression, with SWD appearance being determined by other mechanisms, for instance, corticothalamic connectivity mechanisms in the particular hemisphere. We have to notice that this outcome is quite preliminary and the issue cannot be solved in the frames of the current study. Simultaneous measurement of both thalamic and cortical channels in both hemispheres are necessary to study this issue properly.

Since we had only two channels, we used only methods for pairwise signal analysis. If more signals were obtained, the special additional techniques to distinguish between direct and mediated coupling [Chen et al., 2004; Kornilov and Sysoev, 2018] should be used when applying Granger causality. For phase synchronization index and mutual information function such approaches are not relevant due to they measure the signal similarity regardless its nature rather than directed connectivity.

Also we have to notice that there is no full confidence that results obtained from PTZ rat models can be completely extrapolated to other animal models of SWDs including genetic models as well as to humans. The additional research is strictly necessary to reveal the possible differences. There are two arguments supporting that the achieved results can be extended outside of the scope of the current investigation. First, the investigated SWDs were detected by an automatic procedure [Ershova et al., 2023]. The same algorithm easily detects most SWDs for WAG/Rij and GAERS rats, which supports that the considered SWDs from the point of view of signal shape, spectrum and structure are the same as in genetic rat models. This also let us use the parameters of the Granger causality method very similar to those used previously when studying SWDs of WAG/Rij rats. Nevertheless, we performed the complete model parameter fitting as it was proposed in Ref. [Sysoeva and Sysoev, 2012; Sysoeva et al., 2014] for these data independently. Second, when comparing prediction improvement values for intercortical interactions obtained for SWDs and baseline activity we observed the increase during SWDs similar to the increase detected previously for WAG/Rij rats [Sysoeva et al., 2016c; Sysoeva et al., 2016a], though the papers [Sysoeva et al., 2016c; Sysoeva et al., 2016a] studied different cortical regions within the same hemisphere while we analyzed connectivity between the same (homotopic) regions of different hemispheres.

We also have to notice that the applied approaches use an indirect assumption that the studied signals can be interpreted as time series of some nonlinear oscillators. Such an assumption is common for most studies [Gerster et al., 2020]. However, the question whether the summary activity of the neurons measured as local field potentials may be interpreted in this way is still open. We base our study on the results of the modeling works, specially designed for absence epilepsy [Medvedeva et al., 2018; Medvedeva et al., 2020], which show that Granger causality method applied to model series demonstrates results similar to those applied to experimental ones. Another, earlier papers declare that the EEG can be considered as a liner noisy like signal [Pijn et al., 1991; Frank et al., 1999], but this seems to be applicable to surface encephalograms of healthy subjects only. We have to notice that the role and usefulness of the noise in modeling brain activity is still very unclear, with different aspects considered in the literature, including intristic noise in the equations for a signle neuron [Acebrón et al., 2004] and common noise as an external input [Novichkova et al., 2025].

Acknowledgements

The research was supported by Russian Science Foundation (project No. 25-12-00176, https://rscf.ru/project/25-12-00176/)

References

Acebrón, J. A., Bulsara, A. R., and Rappel, W.-J. (2004). Noisy fitzhugh-nagumo model: From single elements to globally coupled networks. *Physical Review E*, **69** (2), pp. 026202.

Babich, N., Chen, O., Chulkin, V., Marzel, E., Rybalko, A., and Fradkov, A. (2025). Outline of cybernetical neuroscience. *Cybernetics and Physics*, **14** (1), pp. 13– 18.

Berg, A., Berkovich, S., Brodie, M., Buchhalter, J., Cross, J., van Emde Boas, W., Engel, J., French, J., Glauser, T., Mathern, G., Moshe, S., Nordli, D., Plouin, P., and Scheffer, I. (2010). Revised terminology and concepts for organization of seizures and epilepsies: report of the ILAE Comission on Classi-

- fication and Terminology. *Epilepsia*, **51** (4), pp. 676–685.
- Chen, Y., Rangarajan, G., Feng, J., and Ding, M. (2004). Analyzing multiple nonlinear time series with extended Granger causality. *Physics Letters A*, **324**(1), pp. 26–35.
- Coenen, A. M. L. and van Luijtelaar, G. (2003). Genetic animal models for absence epilepsy: a review of the WAG/Rij strain of rats. *Behavioral Genetics*, **33**, pp. 635–655.
- Dolinina, A. Y., Sysoeva, M. V., van Rijn, C. M., and Sysoev, I. V. (2024). Frequency synchronization reveals that spike-wave discharges in WAG/Rij rats are significantly nonlinear phenomenon. *Journal of Biological Systems*, **32**(1), pp. 239–250.
- Ershova, A., Suleymanova, E., Grishchenko, A., Vinogradova, L., and Sysoev, I. (2023). Interhemispheric symmetry and asymmetry of absence type spikewave discharges caused by systemic administration of pentylenetetrazole. *Journal of Evolutionary Biochemistry and Physiology*, **59** (1), pp. 293–301.
- Frank, T. D., Daffertshofer, A., Beek, P. J., and Haken, H. (1999). Impacts of noise on a field theoretical model of the human brain. *Physica D: Nonlinear Phenomena*, **127** (3), pp. 233–249.
- Gerster, M., Berner, R., Sawicki, J., Zakharova, A., Škoch, A., Hlinka, J., Lehnertz, K., and Schöll, E. (2020). Fitzhugh–nagumo oscillators on complex networks mimic epileptic-seizure-related synchronization phenomena. *Chaos: An Interdisciplinary Journal of Nonlinear Science*, **30** (12).
- Hesse, R., Molle, E., Arnold, M., and Schack, B. (2003). The use of time-variant EEG Granger causality for inspecting directed interdependencies of neural assemblies. *Journal of Neuroscience Methods*, **124**, pp. 27–44.
- Huang, N. E., Shen, Z., Long, S. R., Wu, M. C., Shih,
 H. H., Zheng, Q., Yen, N.-C., Tung, C. C., and Liu,
 H. H. (1998). The empirical mode decomposition and the hilbert spectrum for nonlinear and non-stationary time series analysis. *Proceedings of the Royal Society of London*, 454, pp. 903–995.
- Klioueva, I., van Luijtelaar, E., Chepurnova, N., and Chepurnov, S. (2001). Ptz-induced seizures in rats: effects of age and strain. *Physiology & Behavior*, **72** (3), pp. 421–426.
- Kornilov, M. V., Medvedeva, T. M., Bezruchko, B. P., and Sysoev, I. V. (2016). Choosing the optimal model parameters for Granger causality in application to time series with main timescale. *Chaos, Solitons & Fractals*, **82**, pp. 11–21.
- Kornilov, M. V. and Sysoev, I. V. (2018). Recovering the architecture of links in a chain of three unidirectionally coupled systems using the Granger-causality test. *Technical Physics Letters*, **44** (5), pp. 445–449.
- Kozachenko, L. F. and Leonenko, N. N. (1987). Sample estimate of the entropy of a random vector. *Problems of Information Transmission*, **23** (2), pp. 9–16.

- Kraskov, A., Stögbauer, H., and Grassberger, P. (2004). Estimating mutual information. *Physical Review E*, **69**, pp. 066138.
- Kugiumtzis, D. (1996). State space reconstruction parameters in the analysis of chaotic time series the role of the time window length. *Physica D: Nonlinear Phenomena*, **95**(1), pp. 13–28.
- Lüttjohann, A. and van Luijtelaar, G. (2012). The dynamics of cortico-thalamo-cortical interactions at the transition from pre-ictal to ictal LFPs in absence epilepsy. *Neurobiology of Disease*, **47**, pp. 47–60.
- Lüttjohann, A. and van Luijtelaar, G. (2015). Dynamics of networks during absence seizure's on- and offset in rodents and man. *Frontiers in Physiology*, **6**, pp. 16.
- Marescaux, C., Micheletti, G., Vergnes, M., Depaulis, A., Rumbach, L., and Warter, J. (1984). A model of chronic spontaneous petit mal-like seizures in the rat: comparison with pentylenetetrazol-induced seizures. *Epilepsia*, **25** (3), pp. 326–331.
- Marinazzo, D., Pellicoro, M., and Stramaglia, S. (2006). Nonlinear parametric model for Granger causality of time series. *Physical Review E*, **73**, pp. 066216.
- Medina, A. E., Manhães, A. C., and Schmidt, S. L. (2001). Sex differences in sensitivity to seizures elicited by pentylenetetrazol in mice. *Pharmacology Biochemistry and Behavior*, **68** (3), pp. 591–596.
- Medvedeva, T. M., Sysoeva, M. V., Lüttjohann, A., van Luijtelaar, G., and Sysoev, I. V. (2020). Dynamical mesoscale model of absence seizures in genetic models. *PLoS ONE*, **15**, pp. e239125.
- Medvedeva, T. M., Sysoeva, M. V., van Luijtelaar, G., and Sysoev, I. V. (2018). Modeling spike-wave discharges by a complex network of neuronal oscillators. *Neural Networks*, **98**, pp. 271–282.
- Mormann, F., Lehnertz, K., David, P., and Elder, C. E. (2000). Mean phase coherence as a measure for phase synchronization and its application to the eeg of epilepsy patients. *Physica D: Nonlinear Phenomena*, **144**, pp. 358–369.
- Myslobodsky, M. and Rosen, J. (1979). Hemispheric asymmetry of pentamethylenetetrazol-induced wavespike discharges and motor imbalance in rats. *Epilepsia*, **20** (4), pp. 377–386.
- Novichkova, V. A., Rybalova, E. V., Ponomarenko, V. I., and Vadivasova, T. E. (2025). Influence of coupling topology and noise on the possibility of frequency tuning in ensembles of fitzhugh–nagumo oscillators. *Izvestiya VUZ. Applied Nonlinear Dynamics*, **33** (2), pp. 266–282.
- Packard, N., Crutchfield, J., Farmer, J., and Shaw, R. (1980). Geometry from a time series. *Physical Review Letters*, **45**, pp. 712–716.
- Paxinos, G. and Watson, C. (2006). *The Rat Brain in Stereotaxic Coordinates, 6th Edition*. Academic Press, San Diego.
- Pijn, J. P., Van Neerven, J., Noest, A., and Lopes da Silva, F. H. (1991). Chaos or noise in eeg signals; de-

- pendence on state and brain site. *Electroencephalog-raphy and Clinical Neurophysiology*, **79** (5), pp. 371–381.
- Plotnikov, S. A. (2024). Identification of neural mass network parameters using eeg evoked potential data. *Cybernetics and Physics*, **13** (4), pp. 296–301.
- Russo, E., Citraro, R., Constanti, A., Leo, A., Lüttjohann, A., van Luijtelaar, G., and De Sarro, G. (2016). Upholding WAG/Rij rats as a model of absence epileptogenesis: Hidden mechanisms and a new theory on seizure development. *Neuroscience and Biobehavioral Reviews*, **71**, pp. 388–408.
- Scheffer, I. E., Berkovic, S., Capovilla, G., Connolly, M. B., French, J., Guilhoto, L., Hirsch, E., Jain, S., Mathern, G. W., Moshé, S. L., Nordli, D. R., Perucca, E., Tomson, T., Wiebe, S., Zhang, Y.-H., and Zuberi, S. M. (2017). Ilae classification of the epilepsies: Position paper of the ilae commission for classification and terminology. *Epilepsia*, 58 (4), pp. 512–521.
- Schreiber, T. (2000). Measuring information transfer. *Physical Review Letters*, **85**, pp. 461.
- Schwarz, G. (1978). Estimating the dimension of a model. *The Annals of Statistics*, **6**(2), pp. 461–464.
- Smirnov, D. A. (2013). Spurious causalities with transfer entropy. *Physical Review E*, **87** (4), pp. 042917.
- Smirnov, D. A. (2014). Quantification of causal couplings via dynamical effects: A unifying perspective. *Physical Review E*, **90** (6), pp. 062921.
- Solmaz, I., Gürkanlar, D., Gökçil, Z., Göksoy, C., Özkan, M., and Erdoğan, E. (2009). Antiepileptic activity of melatonin in guinea pigs with pentylenetetrazol-induced seizures. *Neurological Research*, **31**(9), pp. 989–995.
- Sysoev, I. V. and Bezruchko, B. P. (2021). Noise robust approach to reconstruction of van der Pol-like oscillators and its application to granger causality. *Chaos*, **31**(8), pp. 083118.
- Sysoeva, M., Sitnikova, E., and Sysoev, I. (2016a). Thalamo-cortical mechanisms of initiation, maintenance and termination of spike-wave discharges at wag/rij rats. *Zhurnal Vysshei Nervnoi Deyatelnosti Imeni I.P. Pavlova*, **66**(1), pp. 103–112.
- Sysoeva, M. V., Dikanev, T. V., and Sysoev, I. V. (2012). Selecting time scales for empirical model construction. *Izvestiya VUZ. Applied Nonlinear Dynamics*, **20** (2), pp. 54–62.
- Sysoeva, M. V., Lüttjohann, A., van Luijtelaar, G., and Sysoev, I. V. (2016b). Dynamics of directional

- coupling underlying spike-wave discharges. *Neuroscience*, **314**, pp. 75–89.
- Sysoeva, M. V., Sitnikova, E., Sysoev, I. V., Bezruchko, B. P., and van Luijtelaar, G. (2014). Application of adaptive nonlinear Granger causality: Disclosing network changes before and after absence seizure onset in a genetic rat model. *Journal of Neuroscience Methods*, **226**, pp. 33–41.
- Sysoeva, M. V. and Sysoev, I. V. (2012). Mathematical modeling of encephalogram dynamics during epileptic seizure. *Technical Physics Letters*, **38** (2), pp. 151–154.
- Sysoeva, M. V., Vinogradova, L. V., Kuznetsova, G. D., Sysoev, I. V., and van Rijn, C. M. (2016c). Changes in corticocortical and corticohippocampal network during absence seizures in WAG/Rij rats revealed with time varying Granger causality. *Epilepsy and Behavior*. **64**, pp. 44–50.
- Turukina, L. V. (2024). Parametric interaction of modes in the presence of quadratic or cubic nonlinearity. *Izvestiya VUZ. Applied Nonlinear Dynamics*, **32**(1), pp. 11–30.
- Vakorin, V., Mišić, B., Krakovska, O., Bezgin, G., and McIntosh, A. (2013). Confounding effects of phase delays on causality estimation. *PLoS ONE*, **8**(1), pp. e53588.
- van Luijtelaar, E. L. and Coenen, A. M. (1986). Two types of electrocortical paroxysms in an inbred strain of rats. *Neuroscience Letters*, **70**, pp. 393—397.
- van Rijn, C. M., Gaetani, S., Santolini, I., Badura, A., Gabova, A., Fu, J., Watanabe, M., Cuomo, V., van Luijtelaar, G., Nicolett, F., and Ngomba, R. T. (2010). WAG/Rij rats show a reduced expression of CB1 receptors in thalamic nuclei and respond to the CB1 receptor agonist, R(+)WIN55,212-2, with a reduced incidence of spike-wave discharges. *Epilepsia*, **51** (8), pp. 1511–1521.
- Vergnes, M., Marescaux, C., Depaulis, A., Micheletti, G., and Warter, J. (1987). Spontaneous spike and wave discharges in thalamus and cortex in a rat model of genetic petit mal-like seizures. *Experimental Neurology*, **96**, pp. 127–136.
- Virtanen, P., Gommers, R., Oliphant, T. E., Haberland, M., Reddy, T., Cournapeau, D., Burovski, E., Peterson, P., Weckesser, W., Bright, J., et al. (2020). Scipy 1.0: fundamental algorithms for scientific computing in python. *Nature methods*, 17 (3), pp. 261–272.